Solar Energy 272 (2024) 112490

Contents lists available at ScienceDirect

Solar Energy

journal homepage: www.elsevier.com/locate/solener

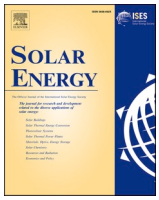

Detection of tracker misalignments and estimation of cross-axis slope in photovoltaic plants

M. López

Department of Mechanical Engineering and Energy, University Miguel Hernandez, Elche 03202, Spain

ARTICLE INFO

Keywords:
Photovoltaic
Single-axis tracking
Shading
Backtracking
Terrain slope

ABSTRACT

Photovoltaic (PV) energy production is becoming a more significant part of the energy mix world-wide due to its clean origin, supportive and cost reductions. Therefore, it is increasingly important to develop methodologies to improve efficiency and reduce energy losses. Solar tracking is a way of increasing the irradiance over the PV field and, subsequently, boosting energy production. Both single-axis and double-axis tracking systems (SATS & DATS) are well known methods but both require not only a proper estimation of the sun's position but also precise knowledge of the tracker's position and orientation. Several factors (construction, design, configuration) can cause the values used to calculate the optimal tracking to be inaccurate, thus increasing production losses. This paper proposes a methodology to calculate the actual orientation of the trackers' axis based on the energy production of its associated strings. Additionally, it provides the height differences between adjacent trackers by detecting shading patterns. This information is key to defining more efficient tracking and backtracking strategies the avoid row-to-row shading and, overall increasing energy production. The proposed method is applied to a real 5 MW facility, identifying misalignments of several degrees in most trackers that were causing annual losses (1 %), not only due to inaccurate tracking but also row-to-row shading.

1. Introduction

With the world's electricity demand rising at an annual rate of 2–3 % [1], there is a growing need to adopt cleaner and more sustainable approaches to meet this demand. Investments in clean energy have risen by 40 % since 2020 [2]. Environmental regulations are directing us towards the use of renewable energy sources, such as wind and solar power, for electricity generation. Solar photovoltaic (PV) technology stands out as a compelling solution to reconcile our increasing electricity demands with environmental constraints. Its simplicity, low-maintenance characteristics, and scalability make it particularly attractive [3]. Moreover, it is abundantly available worldwide.

1.1. Solar tracking

Solar tracking is a crucial aspect in photovoltaic efficiency. Its relevance stems from one of the most fundamental characteristics of solar energy: variability. The relative motion between the Earth and the Sun results in periodic variations on a yearly and, naturally, daily basis. Since, most of the solar radiation reaching the surface comes directly from the solar disc, accurate tracking of its position is necessary for efficient capture of solar energy [4,5].

The ideal orientation of a tracking system can be determined in two ways: either by using irradiance sensors to guide the tracker or by employing mathematical calculations based on astronomical equations that determine the relative position of the Earth and the Sun. Additionally, an irradiance model is necessary to account for diffuse radiation [6]. The use of sensors increases the complexity of the tracker but it is more robust to minor inaccuracies. Conversely, a calculated tracker is unable to correct small errors but it is a more cost-effective option. The proposed technique is applicable to the calculated tracker.

Solar tracking can systems can be grouped in two main categories. Single-axis tracking systems (SATS) rotate the module around a single fixed axis, while a double-axis tracking system (DATS) allows for rotation around two different axes. Consequently, DATS enable the panel to be oriented to any point in the sky's hemisphere, with the only restrictions being the maximum angles of the tracking device. [5–7] provide a comprehensive review of the gains that DATS can obtain over fixed systems (15–50 % [8–11]) and SATS (5–17 % [12,13]). In [14], an average gain of 11 % is reported when comparing SATS with fixed system, while a difference of 5.53 % is found in [15]. Generally, these gains depend mostly on latitude [16,17] and cloud coverage [18]. Therefore, the economic decision on which tracker is best is site-

E-mail address: m.lopezg@umh.es.

https://doi.org/10.1016/j.solener.2024.112490
Received 21 December 2023; Received in revised form 8 March 2024; Accepted 23 March 2024
Available online 28 March 2024

Nomenclature

α	Azimuth of tracker axis [°]
γ	Tilt of tracker axis [°]
β	Angle of incidence [°]
ε	Tracking angle [°]
$\vec{u_z}$	Unit vector normal to the panel.
$\vec{s}$	Position of the Sun (fixed reference)
φ	Azimuth of the Sun
θ	Elevation of the Sun
G_H	Global horizontal irradiance
β_c	Cross-axis slope
$\vec{s'}$	Position of the Sun (tracker reference)
ε_{opt}	Optimal tracking angle
G_{POA}	Irradiance on the plane of array
G_d	Direct irradiance
$G_{s\ d}$	Diffuse sky irradiance
$G_{g\ d}$	Diffuse ground irradiance
α_T	Temperature power coefficient
ΔT_{MU}	Panel temperature minus reference
η_{MU}	Efficiency coefficient of MU

dependent.

As mentioned earlier, the primary component of global irradiance comes directly from the solar disc. [19] provides a theoretical analysis using different irradiance models, indicating that a more horizontal orientation may result in a larger energy yield during specific times. This holds true if the cloud coverage is low, as heavily overcast skies could evenly distribute irradiance over the entire hemisphere. In [20], it was found that an increase of up to 50 % could be achieved if panels were horizontal. Following this idea, there have been other studies developing tracking strategies for SATS that aim to optimize energy yield under cloudy conditions. [18] provides a study across Europe of how a horizontal orientation under cloudy conditions could increase energy production from 1.21 % to 3.01 %, depending heavily on the weather and latitude of the site. The presence of snow on the ground diminishes this effect due to the increase in albedo [17]. A common challenge for these strategies is the forecast of cloudiness, as trackers may take several minutes to reach the target orientation.

Another reason to avoid direct tracking is row-to-row shading [21]. Increasing the distance between rows can eliminate shading, but it comes with a clear increase in land costs. Therefore, backtracking is a common technique to balance both losses. In [22], a method is provided for modelling and identifying shading from production data, showing that even small shading can cause significant losses. The geometry of the trackers is crucial for developing the correct backtracking strategy. A slope-aware methodology is presented in [23]. It allows the calculation of the tracking angle to avoid shading between adjacent trackers on a slope (or at different heights). While the aforementioned study tracked the position of the sun, in [24] a methodology for maximizing irradiance considering diffuse components, is proposed. This methodology allows any slope on the terrain and also covers backtracking by calculating the minimum change in the inclination angle that would avoid shading between rows.

Other tracking methodologies include quantized tracking [25], in which the number of positions of the tracker is limited to a given amount of steps to minimize mechanical wear claiming that with 7 steps the tracker would get 99.27 % of the irradiance. Furthermore, examples of tracking systems using sensors in a closed-loop can be found in [5] but they are not reviewed here as the proposed methodology does not apply to such cases.

1.2. Motivation

The methods presented earlier offer various approaches to determining the optimal angle of inclination of a horizontal SATS under diverse conditions of latitude, weather, cloudiness or even terrain slope. One necessary input for all of them is the actual orientation, land distribution and dimensions of the trackers. This is very relevant information While this information is generally known, it may not be as precise and accurate as desired. In plants using concentrator technologies, the allowed error in tracking is reduced due to the nature of the energy harvesting process. Therefore, calibration methods are already defined [26,27]. Another PV application in which solar tracking is more relevant is in-orbit collectors [28]. However, the techniques described in these papers incur excessive costs for a regular PV plant. To the author's knowledge, there are no other proposed techniques to obtain these values without expensive field measurement, even though their effect on energy production and on the development of tracking and backtracking strategies is well established [24,29,30].

1.3. Contribution

The main contribution of the research is a methodology to calculate the actual orientation of each tracker's axis (azimuth and tilt) using readily available data series such as produced power and tracker inclination. Additionally, it provides a simple method to calculate the height differences between adjacent trackers along each line of trackers due to a cross-axis slope. This information is necessary to determine tracking and back-tracking profiles for each tracker of the plant. The industry benchmark to obtain this information is through field measurement during construction. However, as shown in this paper, these values may not be accurate enough to generate optimal tracking and backtracking strategies. The methodology is applied to a real facility in Spain, revealing significant misalignment in most of the trackers and avoidable row-to-row shading due to differences in heights not considered in the backtracking strategy. The application of the methodology results in a 0.9 % increase in annual energy production due to the elimination of row-to-row shading and improved tracking. In addition to this gain, the reference values for monitoring production can also be enhanced, providing a better monitoring system. Another advantage of the proposed methodology is that its input data is limited to production data so its application does not have any extra costs.

The paper is organized as follows: Section 2 describes the plant and the data used, as well as the methodology to obtain and validate both true tracker orientation and height profiles. This section also includes the model for power production at a string level and the tracking and backtracking strategies that make used of the calculated parameters. Section 3 provides the results for the validation of the model, the actual orientations, and height profiles found, as well as the different losses eliminated. Finally, section 4 includes the conclusions and future work.

2. Materials and methods

2.1. Plant description

The facility used in the analysis is located in the center of Spain but its exact location cannot be disclosed. The plant has a peak power of 5MWp comprised of 2 inverters with 252 strings each. Each string has 30 modules that are mounted on single-axis trackers with capacity for 30, 60 or 90 modules. The tracking system is a horizontal single axis and its tracking angle, ε, is defined as 0 when the tracker is horizontal. The maximum tracking angle is 55°. The trackers are arranged in lines parallel to a North-South axis with a row pitch of 7.8 m and a tracker width of 3 m. Therefore, the Ground to Cover Ratio (GCR) is 0.385. This configuration is illustrated in Fig. 1, showing a 3d representation of three trackers along with their plan and elevation representations. The plan shows the misalignment of the tracker axis with the North-South

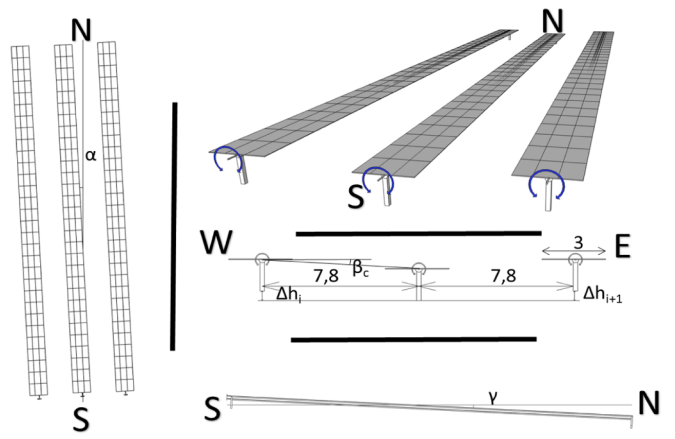

Fig. 1. 3d representation of 3 trackers. Plan and elevation view of the trackers to illustrate the three types of misalignments detected: α, γ and Δh.

axis (α). The East-West elevation shows the differences in heights (Δh) detected by the algorithm and the cross-axis slope (β_c). The North-South elevation shows the misalignment of the tracker axis with the horizontal plane (γ). The concept of cross-axis slope is well defined in [23] and it essentially represents the angle between a horizontal plane and a vector perpendicular to the tracker's axis and pointing to the axis of the next tracker.

In this manner, each tracker can be shaded by one tracker on the morning and by another one on the evening with the only exception of trackers located at the boundaries. The initial assessment of external shadings showed that there was not a significant power loss due to this phenomenon. The more thorough analysis carried out during this research found no shading losses other than the row-to-row shading reported in its findings. An approximate arrangement is shown in Fig. 2a. The horizontal position and vertical length of line of trackers tracker has been modified to maintain anonymity of the plant but the amount of trackers in each line is accurate.

The monitoring system provides information at a two-string level. Therefore, each monitoring unit (MU) actually represents 2 field strings. Monitoring units have a peak-power of 19.8kWp and are named with five digits (IBBSS) identifying the inverter, the box and the string. This means that a single MU can occupy the following positions:

- A full 30 module tracker plus the top or bottom row of a 90-module tracker.
- A full 60 module tracker.
- The top and middle rows of a 90-module tracker.
- The bottom and middle rows of a 90-module tracker.
- The top and bottom rows of different 90-module trackers.

The different configuration of strings on a tracker is shown in Fig. 2b.

2.2. Data description

The data needed to apply this methodology is easily accessible on any PV facility. The power is logged in 252 series, each representing the power from two field strings. The tracker angle from all 187 trackers is also used also with a granularity of 5 min. The panel temperature is measured in one of the panels and it is used as a proxy for panel temperature of all panels. Additionally, a locally calibrated pyranometer measures global horizontal irradiance. Plant's latitude, longitude and altitude along with time stamps from the rest of the data series are used to calculate all derived variables.

2.3. Calculation of theoretical orientation of the trackers

The proposed methodology is inherently data-driven. To this end, some of the reported information about the plant will be tested and confirmed by the monitored data. This section focuses on confirming the orientation (azimuth and tilt) of the tracker's axis used in the plant setup.

The plant has reported that the trackers are oriented on a flat surface (tilt of the tracking axis, γ, is equal to 0°) and following a North-South axis (azimuth of the tracking axis, α, is also equal to 0°). Additionally, the current backtracking strategy assumes that the cross-axis slope is also zero and all trackers are at the same height. These parameters are used to develop a tracking strategy aimed at minimizing the angle β between the incident solar beam and the vector normal to the module (u_z''). This strategy is typical for SATS on a horizontal plane [23].

The angle of incidence is minimized by pointing the vector u_z'' in the direction of the sun's projection on the plane perpendicular to the tracker's axis. The optimal value for tracking angle, ε_{opt}, can then be calculated by obtaining the position of the sun in the coordinate system of the tracker. This change of reference is more easily calculated using

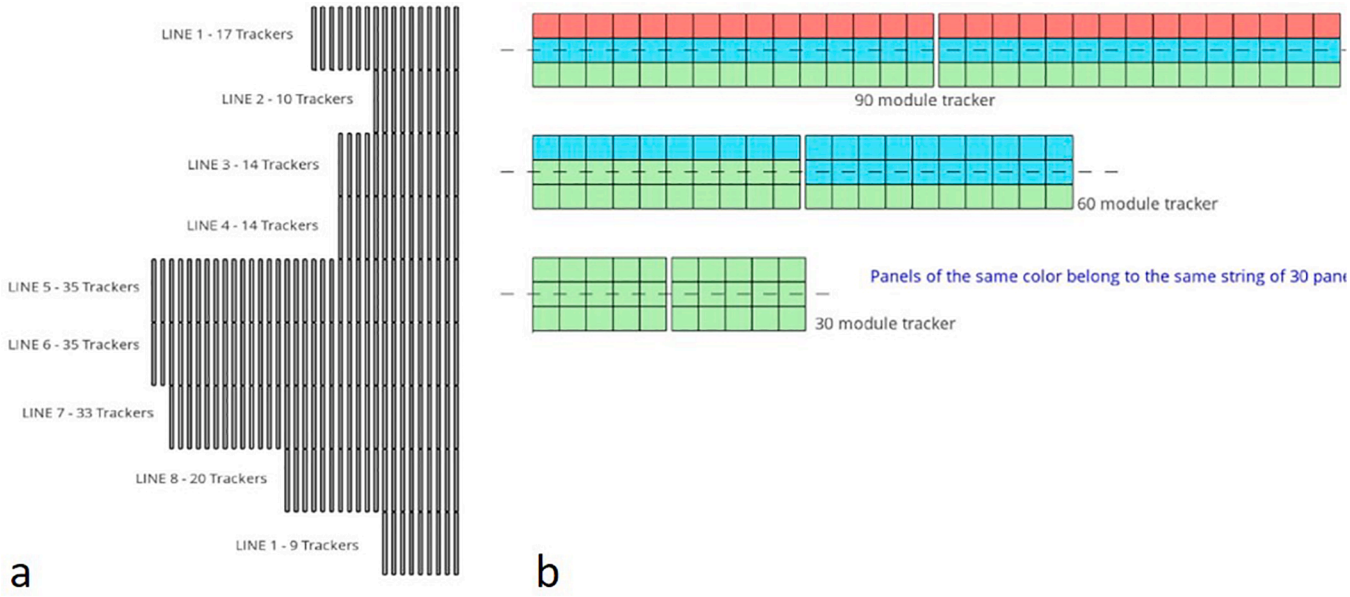

Fig. 2. a) distribution of trackers in lines. b) distribution of strings on trackers of different size.

Cartesian coordinates (1).

$$\begin{bmatrix} s_x \\ s_y \\ s_z \end{bmatrix} = \begin{bmatrix} -\cos\theta \bullet \cos\varphi \\ \cos\theta \bullet \sin\varphi \\ \sin\theta \end{bmatrix} \quad (1)$$

These coordinates can then be rotated to the desired reference by matrix multiplication (2).

$$R_y = \begin{bmatrix} \cos\gamma & 0 & \sin\gamma \\ 0 & 1 & 0 \\ -\sin\gamma & 0 & \cos\gamma \end{bmatrix} R_z = \begin{bmatrix} \cos\alpha & \sin\alpha & 0 \\ -\sin\alpha & \cos\alpha & 0 \\ 0 & 0 & 1 \end{bmatrix} \begin{bmatrix} s_x' \\ s_y' \\ s_z' \end{bmatrix} = R_z \bullet R_y \bullet \begin{bmatrix} s_x \\ s_y \\ s_z \end{bmatrix} \quad (2)$$

$$\varepsilon_{opt} = \tan^{-1}\left(-s_y'/s_z'\right) \quad (3)$$

The ideal tracking angle (ε_{opt}) is easily obtained using (3). Note that all signs are assigned so that the angles γ, α and ε are positive as they are shown in Fig. 3.

Nevertheless, our goal is to reverse this process and reveal the tilt and azimuth parameters that fit the tracking strategy best. The fitting process was done by minimization of the quadratic error between the series of actual tracking angle and that of a theoretical tracking angle with elevation and azimuth as parameters. The results shown on Table 1 confirm that the initial configuration of the plant was based on the 0° inclination and 0° azimuth assumption.

2.4. Calculation of actual orientation

The central concept of this paper is the feasibility of determining the actual inclination and azimuth of the trackers by analyzing their power generation. Fig. 4 shows how irradiance on a tracker's surface is different if their orientation is different. Changes in both azimuth and tilt angles of the tracker's axis lead to noticeable shifts in irradiance. This section outlines the steps to determine the orientation of a tracker from its power generation, subsequently used to assess the optimality of its tracking strategy.

a) Model for the power generation.

An equation for modeling the output of a solar array is provided in [21]. Eq. (4) includes a term (η_{MU}) to account for specific behavior of each MU:

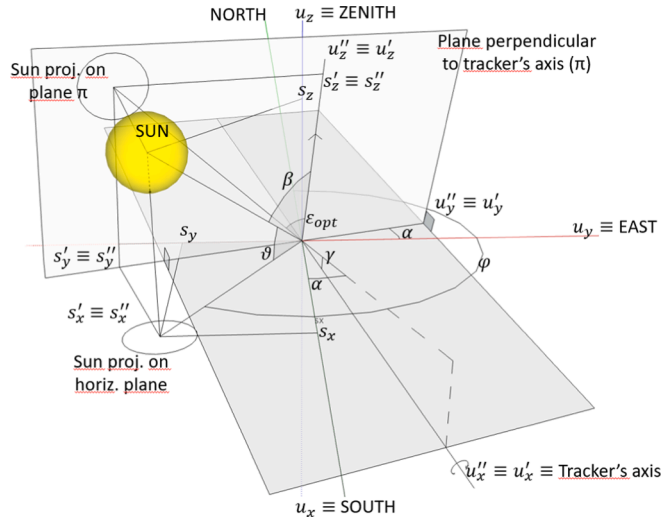

Fig. 3. Position of sun and solar panel. The fixed reference system (u) is horizontal and North-South oriented. For clarity reasons, the un-rotated tracker reference system (u') and the tracker reference system (u'') coincide but u'' can rotate around the tracker's axis.

Table 1
Calculated values for the orientation of trackers.

Variable	Mean	Std. Dev.
Azimuth (deg.)	0,08	0,02
Tilt (deg.)	0,14	0,1

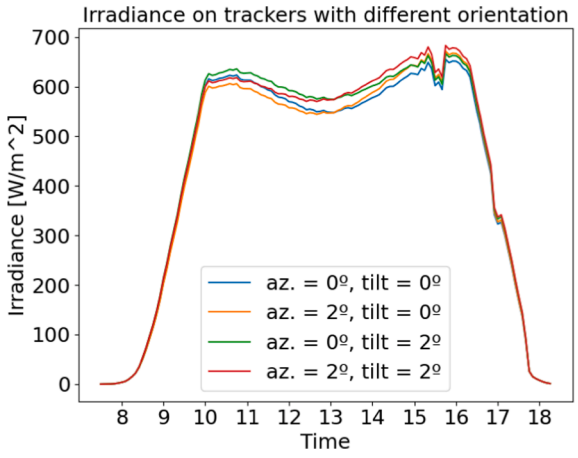

Fig. 4. Simulated irradiance on the plane of one tracker using the Perez model considering different azimuth and tilt angles for the tracker's axis.

$$P_{MU} = P_{MU}^{*} \bullet \frac{G_{POA}}{G^{*}} \bullet (1 - \alpha_T \bullet \Delta T_{MU}) \bullet \eta_{MU} \quad (4)$$

Where P_{MU}* is the nominal power of the array and G* is 1000 W / m^2. Irradiance on the plane of array can then be broken down as seen in eq. (5), which follows the Perez model [31].

$$G_{POA} = G_d + G_{sd} + G_{gd} \quad (5)$$

$G_{s\,d}$ and $G_{g\,d}$ are the diffuse irradiance from the sky and from the ground respectively and they are calculated using the Perez model implemented in *pvLib* using G_H as an input. The albedo coefficient is assumed to be 0.25. The following paragraphs will provide the details of the measured and calculated variables that take part in the model as long as the parameters the will be used to fit the model to the data.

b) Measured data.

Meteorological variables: The only irradiance measured is global horizontal irradiance (G_H) with a granularity of 5 min. Module temperature is approximated using data from one sensor located in one of the modules and applied across all trackers. While wind information was initially considered, it was ultimately excluded as it did not contribute to improving the model's accuracy.

Electrical variables: Power from each of the MUs is measured at 5-minute intervals. Each tracker is assigned a MU fully located on that tracker, except for 30-module trackers that cannot accommodate a full MU. In these cases, the MU containing the field string on the tracker is used. While the results may be influenced by the other half of the MU located on a nearby tracker, this situation only represent about 3 % of the total power generation.

Tracking variables: The tracking angle (ε) of each tracker is reported using two variables: set point and actual value. However, the actual value series exhibited anomalies during periods of undisturbed power generation. Consequently, the actual value was discarded in favor of the set point. This approach may result in instances of low production, as the actual angle may not precisely match the set point, but none were identified in the dataset.

Time: Timestamps for all data points are also used to synchronize plant data to solar position.

c) Calculated data.

Solar position: Solar elevation and azimuth is calculated using the python library *pvLib* using as parameters the time, latitude and longitude of the plant.

Tracker orientation: The orientation of the tracker is commonly specified as a pair of azimuth and tilt angles of the panel. Alternatively, the same information can be expressed by providing the azimuth and tilt of the tracker's axis along with the tracking angle. The former provides a sense of how the array is oriented at any moment while the latter helps understanding how such orientation is achieved. Fig. 3 illustrates the definition of these variables. It is worth noticing that the azimuth and tilt of the tracker's axis are fixed with the tracking angle as a variable. However, both panel's azimuth and panel's tilt are variables.

A straightforward method for calculating the tilt and azimuth of the panel from the azimuth and tilt of the tracker's axis and its tracking angle is to first determine the vector normal to the tracker's surface $u_z^{''}$, and then calculate tilt and azimuth from its components. The matrix rotation shown in Eq. (2) can be used to obtain $u_z^{'}$ from u_z. R_y represents a rotation around the y-axis to account for the axis' tilt and R_z is a rotation around the z-axis for the azimuth. The vector $u_z^{''}$ is subsequently calculated by rotating $u_z^{'}$ around the rotated x'-axis to account for the tracking angle (ε). $R_{x'}$ defined in (6) is a general rotation matrix of an angle ε around vector u. Eq. (7) shows the particularization for a rotation around vector $u_x^{'}$. The full calculation of $u_z^{''}$ is shown in (8) and the final process to obtain the panel's tilt and azimuth is presented in (9).

$$R_x^{'} = \begin{bmatrix} \cos\varepsilon + u_x^2(1-\cos\varepsilon) & u_x u_y(1-\cos\varepsilon) - u_z\sin\varepsilon & u_x u_z(1-\cos\varepsilon) + u_y\sin\varepsilon \\ u_y u_x(1-\cos\varepsilon) + u_z\sin\varepsilon & \cos\varepsilon + u_y^2(1-\cos\varepsilon) & u_y u_z(1-\cos\varepsilon) - u_x\sin\varepsilon \\ u_z u_x(1-\cos\varepsilon) - u_y\sin\varepsilon & u_z u_y(1-\cos\varepsilon) + u_x\sin\varepsilon & \cos\varepsilon + u_z^2(1-\cos\varepsilon) \end{bmatrix} \quad (6)$$

$$u = u_x^{'} \Longrightarrow \begin{bmatrix} u_x \\ u_y \\ u_z \end{bmatrix} = \begin{bmatrix} u_{x,x}^{'} \\ u_{x,y}^{'} \\ u_{x,z}^{'} \end{bmatrix} \quad (7)$$

$$u_z^{''} = R_x^{'} \bullet R_z \bullet R_y \bullet u_z \quad (8)$$

$$\gamma = \cos^{-1}\left(u_z^{''} \bullet u_z\right) \alpha = 90^{\circ} + atan2\left(-u_{z,x}^{''}, -u_{z,y}^{''}\right) \quad (9)$$

Angle of incidence: The angle of incidence (β) refers to the angle between the aforementioned vector normal to the tracker's surface ($u_z^{''}$) and the unit vector pointing to the sun. The calculation of this angle is done as the arccosine of the dot product of both unit vectors.

Irradiance on Plane of Array (G): The Perez model, implemented in *pvLib*, is used for its calculation. This model requires the solar position and tracker orientation as inputs. In addition, diffuse horizontal irradiance and direct normal irradiance are calculated using [32] as implemented in *pvLib*. Other parameters like *airmass* or extraterrestrial normal irradiance where also obtained using *pvLib*. The selected set of Perez coefficients was '*allsitescomposite1990*'.

d) Optimizing parameters.

The modeling of the production of an *MU* requires the estimation of several parameters. The performance coefficient explicitly shown in (4) is obvious on the list but other parameters are hidden within the definition of G_{POA}. The following paragraphs describe these parameters:

Array's performance coefficient (η_{MU}): A performance coefficient is assigned to each tracker to accommodate minor unknown errors. A coefficient deviating significantly from 1 would indicate that the assigned *MU* is performing oddly for unaccounted reasons and the rest of the parameters should be quarantined.

Tracker's axis azimuth and tilt (α, γ): These values will determine the actual orientation of the tracker at each instant along with the measured tracking angle (ε). They represent the deviation from the North-South axis and the inclination of the axis. As a deviation, a value of 0° in azimuth means the tracker is actually North-South aligned, while a positive value of tilt means and inclination towards south or, more precisely, the direction pointed by the azimuth value.

e) Optimizing methodology.

The orientation and performance parameters are obtained through a brute-force approach with a granularity of a tenth of a degree for orientation and 0.1 % for performance. The cost function, defined in Eq. (10), represents the relative RMSE between the expected production, defined in Eq. (4), and the actual production. Since we are calculating the actual orientation of each tracker, a specific *MU* is assigned to represent each tracker.

$$relRMSE = \left(\frac{\sum_{i=1}^{n} y_{real}}{n}\right)^{-1} \sqrt{\frac{\sum_{i=1}^{n}\left(y_{model} - y_{real}\right)^2}{n}} \quad (10)$$

2.5. Calculation of relative height

While it does not affect the angle of incidence, the height of the tracker compared to that of its neighbors can cause row-to-row shading, thereby diminishing power generation. The proposed methodology utilizes this information to determine the most likely relative height of each row, which, in turn, is used to calculate a proper backtracking strategy.

To achieve this, each production data point is categorized as low (<85 %) or normal (>85 %), depending on the ratio between its actual and expected yield, or irrelevant (expected power lower than 5 %),

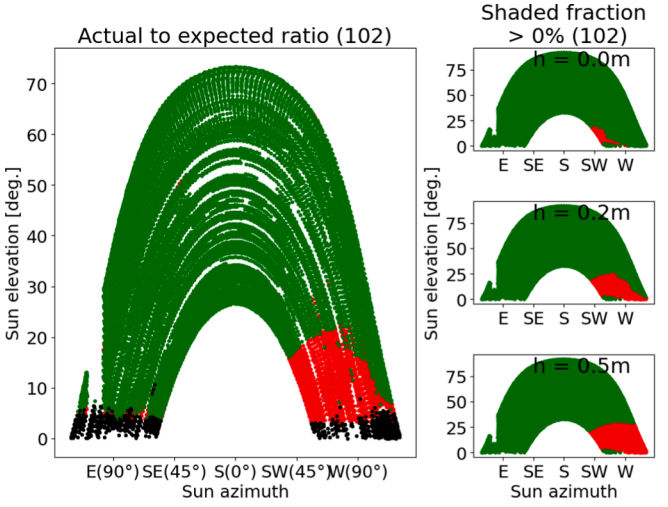

Fig. 5. Cylinder graph of production ratio and shaded tracker for different height difference. In this case, the red points indicating low yield match the red points indicating shaded tracker when the height difference is equal to 0.2 m. (For interpretation of the references to colour in this figure legend, the reader is referred to the web version of this article.)

based on its expected yield. Additionally, the geometry of the trackers is used to determine the shaded fraction of each tracker as a function of the position of the sun and hypothetical height difference. All data points are categorized as shaded or unshaded for different heights ranging from 0 to 0.5 m. The matching index, as described in Eq. (11), is obtained for each relative height to which one causes the shade profile most likely to fit the low-power points. These classifications are depicted in Fig. 5 for one of the MUs representing one tracker. Shading causes a very steep decline in power yield, so an 85 % threshold allows to exclude other causes for low production that are less grave (85–95 %) while tracing a very accurate profile of the shaded instants. A threshold of 80 % is used in [22] but a most restrictive value is preferred in this work.

$$m = \frac{n(shaded \cap low)}{n(shaded \cap normal) + n(unshaded \cap low)} \tag{11}$$

The datasets are restricted to points with sun elevation lesser than 15° and sun azimuth greater or lower than 180° depending on whether the shading occurs from the East or the West. The height with the greatest m value is then assigned as height difference between the trackers.

Row-to-row shading can occur during sunrise or sunset. but different part of the tracker's surface will be shaded in each time period. The *MU* representing the tracker should be the one more likely to be shaded, i.e. the one on the lower part of the tracker as it faces the sun. This means that, for each tracker, one *MU* will be used to trace the morning shade, and a different one for the evening shade. The estimated values will then represent the height difference between the shaded tracker and both the tracker on the East and the tracker on the West. In this manner, two values will be obtained for the relative height between two adjacent trackers. The following cases were identified:

- Two zeros: The shaded profile (if any), caused by the trackers to each other, is coherent with both of them being at the same height.
- Zero and positive number: The shaded profile allows to calculate the height difference from one direction but not from the other because shade only occurs either in the morning or the evening. The positive number is taken as the correct value.

The case in which both analysis (from East and West) provide a height difference, while possible, was not encountered.

2.6. Calculation of backtracking strategy

The orientation and height parameters are used to determine the most productive orientation of the trackers. When the sun is sufficiently high, all trackers should point to the sun's projection on the plane perpendicular to the tracker's axis. However, when shading begins to occur, trackers should adopt a more horizontal position to avoid row-to-row shading. The proper strategy for this is well defined in [23] for trackers in a horizontal field (same height) and also for trackers on fields with a constant slope. However, the results for the height of the trackers will show that, even for a small plant like this one, height difference among trackers can vary greatly along a line of rows. The optimal backtracking strategy for this case is beyond the scope of this paper, but in order to apply the results obtained in the parametrization of the plant (orientation and heights) a naive strategy is proposed.

Each tracker is limited on both sides, so two backtracking profiles are obtained for each tracker: one avoiding shades from one side and one from the other. The more restrictive one is used. This is a conservative strategy that, in places with sudden changes in the slope, may cause some losses due to excessive backtracking, but it will definitely avoid shading.

3. Results

In this section, the model will be validated, and the parameters obtained from the optimization process will be presented. In addition, the effect of the misalignments of the axis and the differences in heights found will be quantified. It will be revealed that this effect has two components: one related to the sub-optimal tracking of the sun due to an inaccurate tracking strategy and also one resulting from the row-to-row shading, product of a miscalculated backtracking strategy.

The data used spans a period of two years from which the first year has been used to identify the parameters of the model, determine the possible misalignment present on the plant and develop a new tracking and backtracking strategy. The data from the second year was then used to validate the model and to quantify the effect that the proposed tracking and backtracking strategy would have. The production improvement is based on a simulation as it has not been implemented in the field yet.

3.1. Validation of the model

To apply the model and calculate the parameters, it is essential to establish its own accuracy first. The reported value for the error of the model is the *RMSE* relative to the average as calculated in Eq. (10). The error is calculated using data from all strings for a full year, using the initial assumption of tilt and azimuth and also using the optimized results. To avoid row-to-row shading, backtracking times are excluded from this calculation. Fig. 6 shows an example of the real and modeled series for one day, showcasing the effect of the change in orientation with a more accurate fit.

As shown in Table 2, the error on sunny instants is 5.12 %, and it is reduced to 4.48 % if the correct orientation is considered. The error on cloudy moments is higher because, on many occasions, the clouds do not cover the sensor and the string simultaneously. Overall, due to the low error and the significant reduction achievable with the correct orientation, we consider the model valid for our intended use.

3.2. Orientation of the trackers

The trackers are arranged in a rectangular pattern along 9 lines with different number of rows as shown in Fig. 2a. The orientation results are detailed for each line in Table 3. The obtained values show that the actual azimuth of the tracker's axis is indeed 0° (North-South axis) but the tilt of the axis is approximately −2°. The negative sign means it is actually tilted towards North.

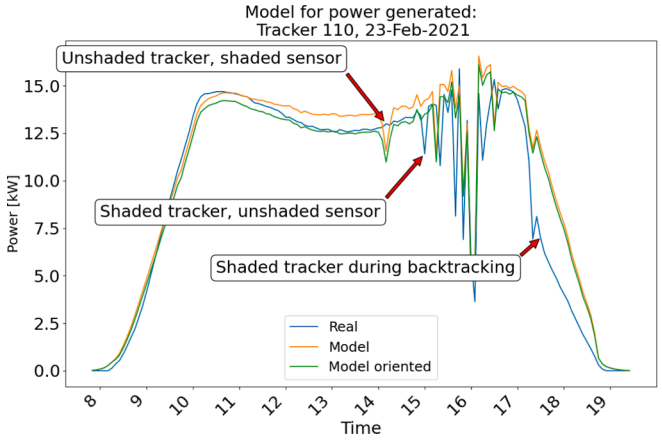

Fig. 6. Power generated by the representing MU (1MU = 19.8kWp) of tracker 110 on Feb. 23rd. The trace representing the model based on the calculated orientation (GREEN) fits the real trace (BLUE) more accurately than the model with the initial orientation (ORANGE). Still, larger errors occur when the piranometer is shaded but the tracker is not and viceversa and, specifically to this tracker, when the tracker gets row-to-row shaded in the evening. (For interpretation of the references to colour in this figure legend, the reader is referred to the web version of this article.)

Table 2
Validation of the model.

	0° tilt / 0° azimuth		ORIENTED	
	All	Sunny	All	Sunny
Mean	8,55 %	5,12 %	7,95 %	4,48 %
Std. dev.	1,47 %	0,92 %	1,44 %	0,84 %

The effect of the difference in axis tilt is a change in the optimal orientation of the tracker. Fig. 7 shows the optimal tracking angles for a single day for both horizontal and tilted axes. The graph demonstrates that even though there is a maximum difference in optimal tracking angle of nearly 3 degrees, the maximum difference in the cosine of the angle of incidence is lower than 0.002. Therefore, very little difference in energy yield can be expected from this change.

Nevertheless, it should not be dismissed the fact that, even if the energy yield does not change significantly, the expected yield does. A tracker that is supposed to have an axis at 0° tilt would have an irradiance 2.6 % higher than one at 4° tilt towards North and up to 8 % on winter days. This means that a monitoring system under the 0° tilt assumption would overestimate energy yield leading to an error on the estimated efficiency of the plant. Even comparing trackers with different tilts may cause the misidentification of underperforming strings.

3.3. Height of the trackers

The methodology to calculate tracker heights provides the relative height between each pair of adjacent trackers on the same line. The entire set of relative heights allows us to define a profile for the line, which can be seen on Fig. 8, where heights are relative to the most Eastern tracker.

The downward slope at the beginning of each line indicate that row-to-row shading is more likely to happen in the evening rather than in the morning. The situation is the opposite when the slope is upwards. It is worth noticing that even if a tracker is shaded, only the string on the bottom part will be affected, as it is very unlikely that the whole tracker is shaded.

Fig. 9 shows the following 6 cases:

- String 10102: String shaded in the evening because its located on the bottom and middle parts of tracker 102, which is second on line 1.
- String 10109: String shaded in the evening because its located on the bottom and top parts of trackers 104 and 105, which are fourth and fifth on line 1.
- String 10110: String unshaded because its located on the top and middle parts of tracker 105.
- String 20103: String shaded in the morning because its located on the bottom and middle parts of tracker 201, which is on the upward slope of line 5.
- String 20111: String shaded in the morning because its located on the bottom and top parts of trackers 202 and 203, which are located following tracker 201.
- String 20109: String unshaded because its located on the top and middle parts of tracker 222, which is on the upward slope of line 6.

3.4. Losses due to orientation

The change in orientation of a particular tracker and the *MUs* fitted onto it alters the irradiance on the plane of the array, subsequently affecting energy production. There are three components of the global irradiance: direct, diffuse from the sky, and diffuse from the ground. The first one is the most relevant and it is maximized by minimizing the

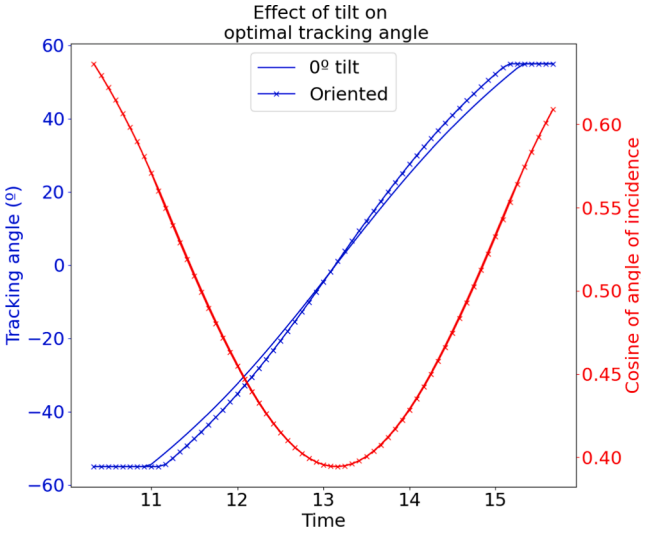

Fig. 7. Tracking angle and correspondent cosine of angle of incidence for a tracker assuming both 0° tilt and azimuth and the calculated angles. The difference in cosine is negligible.

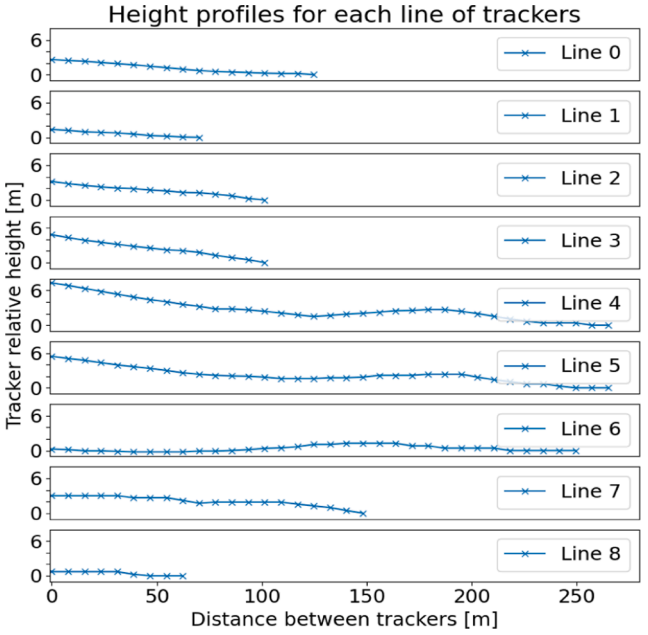

Fig. 8. Height profile of each line of tracker rows.

Table 3
Mean and standard deviation of the tilt and azimuth angle of the tracker's axes grouped by lines of rows.

[deg.]	LINE 1	LINE 2	LINE 3	LINE 4	LINE 5	LINE 6	LINE 7	LINE 8	LINE 9	ALL
Tilt mean	−2,8	−3,9	−1,5	−2,3	−1,6	−1,3	−2,3	−3,4	−2,7	−2,2
Tilt std. dev.	0,8	0,6	0,8	0,9	1,3	0,9	0,7	0,7	0,2	1,2
Azimuth mean	−0,2	−0,2	−0,4	−0,3	−0,2	−0,3	−0,2	−0,4	−0,5	−0,3
Azimuth std. dev.	0,5	0,2	0,4	0,3	0,4	0,3	0,4	0,3	0,4	0,4

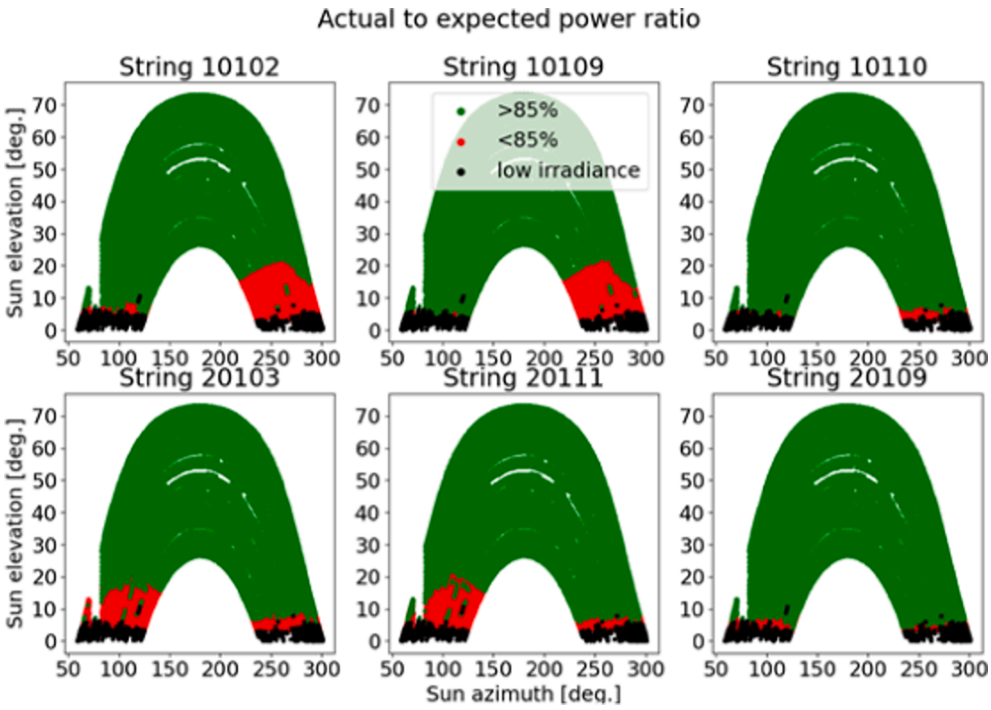

Fig. 9. Production ratio of several strings. Red dots signify low ratio mostly due to shading. When irradiance was too low dots were colored black. (For interpretation of the references to colour in this figure legend, the reader is referred to the web version of this article.)

Table 4
Changes in annual energy yield under new orientation.

	Sunny	Cloudy	All
Morning	0,005 %	0,047 %	0,022 %
Evening	0,135 %	−0,034 %	0,046 %
All	0,062 %	0,002 %	0,034 %

angle of incidence. The second one is maximized when the panel is horizontal and has access to the full sky dome. The third one is maximized when the panel is most inclined (maximum tilt). The changes in orientation proposed optimize direct irradiance, but the other two components are not taken into consideration.

The result of applying the tracking strategy considering the new calculated orientation of the tracker's axis is shown in Table 4. As expected, the improvement is negligible, in part because the change in the angle of incidence is small, but mainly because the change in irradiance depends on the cosine of the angle. Nevertheless, it is worth noticing that the improvement is larger on sunny days than on cloudy days and also in the evening rather than in the morning. The former is because the direct component is larger on sunny days and the latter is due to the larger differences in the new profile. The decrease in production seen in the evenings of cloudy days occurs because the panel is especially more tilted during the evening, and therefore, the sky diffuse irradiance on the plane of array is lower. This is especially relevant on cloudy days when sky diffuse irradiance is more significant. Fig. 10 illustrates these phenomena.

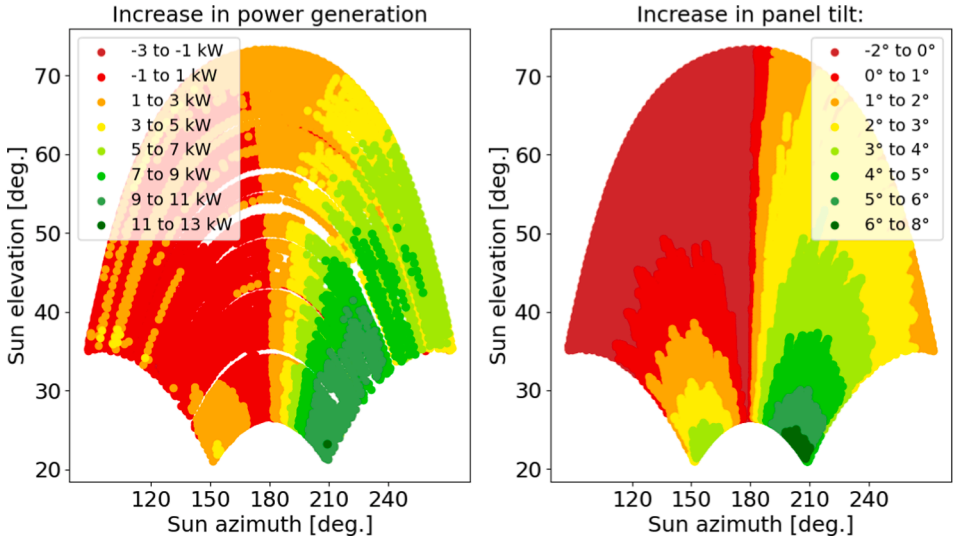

Fig. 10. A) increase in power generation. b) increase in panel tilt. times when the change in tilt is larger provoke larger increments. negative values represent decrement in power generation under the new orientation.

Table 5
Changes in annual energy yield under new backtracking.

	Sunny	Cloudy	All
Morning	14,55 %	9.00 %	11,88 %
Evening	4,63 %	0,46 %	2,55 %
All	7,51 %	2,82 %	5,20 %

3.5. Losses due to row-to-row shading

The height differences estimated on section 3.3 were used to develop new backtracking profiles for each tracker. These profiles allowed the use of our model to simulate the new situation considering the new irradiance associated with the new backtracking profile and assuming that row-to-row shading is avoided. The results are shown in Table 5.

The gains from the new height-aware backtracking amount to a 5.2 % increase in power generation during backtracking. It was expected that power increase during sunny days would be larger than on cloudy days, but it is also remarkable that the biggest gain does not come from avoiding evening shading, which was the most frequent, but from optimizing the morning profile with a more aggressive backtracking. This is because while all strings benefit from the morning profile, only those affected by the evening shade improve their output with the new profile, while the unshaded strings reduce theirs. These phenomena are illustrated in Fig. 11.

Overall, after parametrizing the plant and discovering the true orientation and height profile of the trackers, the new tracking and backtracking strategy, while conservative, still provides a 0.95 % increase in power generation over the whole year. The improvement in production is calculated by comparing the simulation using the previous tracking strategy and another one following the proposed one over the course of the testing year. This improvement in production assumes that the new tracking strategy does not incur in extra power usage by the actuators. The proposed tracking has the same daily trajectory as the current one, differing only on as much as 8 degrees as any given time. In addition, the increase in energy consumption of the actuators has been discarded as irrelevant in comparison to energy production in [18] which described more aggressive changes in the tracking profiles.

4. Conclusions

In this study, we developed a methodology for determining the actual orientation of solar panels within a photovoltaic plant, relying solely on the production data from each string in the plant. Additionally, we successfully calculated the real height differences between various rows of panels. The methodology is cost-effective, requiring only readily available monitoring data such us power generation at the string level, tracking angle of each tracker, panel temperature (one data series to approximate all), and global horizontal irradiance.

The methodology was applied to the data from an active facility in Spain, revealing significant differences between the initially considered tilt and azimuth angles of the tracker's axis and the obtained ones. These differences were primarily in tilt, with discrepancies of up to 4.2 degrees. The calculated orientation for the trackers reduced the modelling error of the plant on sunny instants from 5.12 % to 4.48 %. This improvement indicates that the production data fits the model significantly better when the new orientation is considered.

The altered orientation renders the current tracking strategy obsolete, prompting its readjustment through the established procedure. However, despite causing tilt changes in the trackers exceeding 5 degrees and resulting in a power increase of 0.13 % at certain points, the overall effect is a net gain of 0.034 %. While this improvement might not significant in this specific case, instances with larger errors in orientations would likely yield greater gains. Another crucial application of this methodology lies in string monitoring. Establishing a benchmark for string performance monitoring often assumes identical performance among surrounding strings. This methodology can help uncover consistent differences between similar strings over time, providing a more precise basis for alarms.

The methodology also enabled the determination of the height profile of the tracker rows by analyzing the expected versus actual production ratio of the characteristic strings. The quality of the match between the shaded pattern and the low performance ratio was quantified and used to ascertain the height difference between adjacent trackers. Similar to the orientation findings, the new height profile rendered the existing backtracking strategy obsolete, necessitating the design of a new strategy to eliminate shading on trackers while minimizing the angle of incidence. The revised backtracking not only

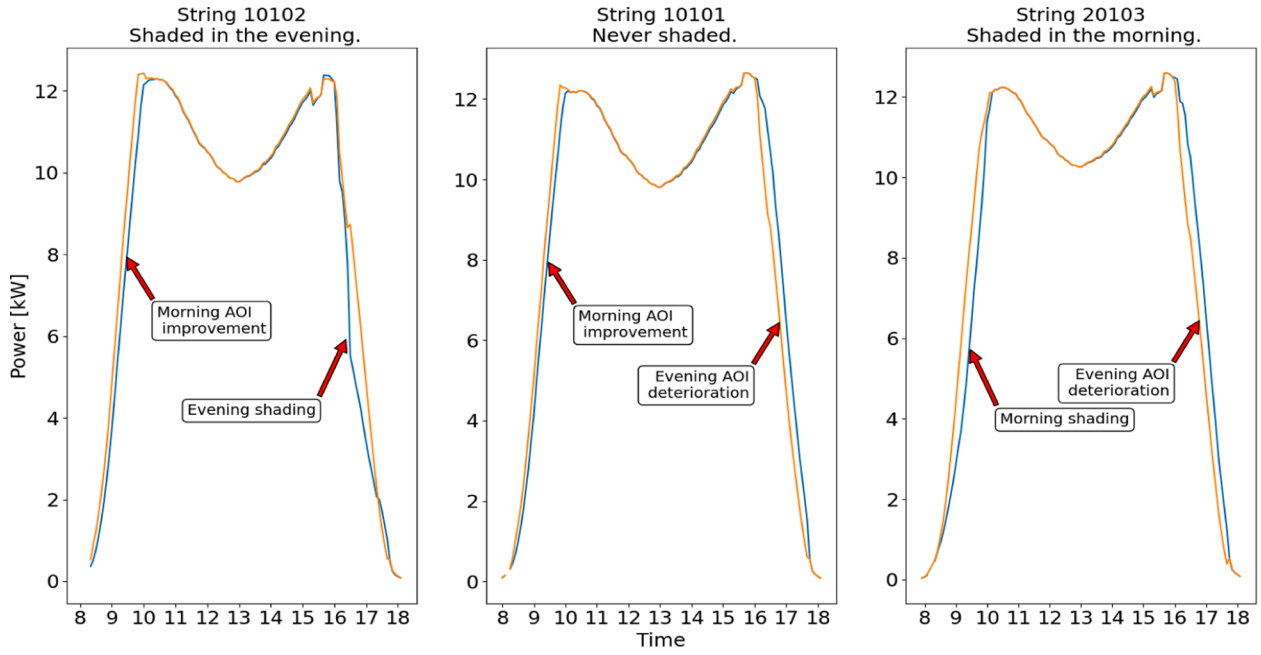

Fig. 11. Power profile of three MUs comparing the effect of the old (blue) and the new (orange) backtracking. (For interpretation of the references to colour in this figure legend, the reader is referred to the web version of this article.)

provided gains from avoiding shading, particularly in the evening due to the east-facing slope, but also from allowing a steeper angle in the morning. The overall increase during backtracking amounted to 5.2 %.

The cumulative gain from both aspects amounts to 0.95 %, achievable directly by reprogramming the tracking profiles. Several other benefits would derive from avoiding shaded panels as it has been documented [22].

Future works will extend the application in two directions: the first one will be to develop optimal strategies to design backtracking on irregularly sloped fields, not only considering the above mentioned aspects of avoiding shades and minimizing angle of incidence but also taking into account that in cloudy conditions, a panel facing up may have a higher yield as some of our results would suggest. The second application will be to introduce individual tracker orientation into string monitoring systems to account for difference in string production due to different plane of array irradiance.

Declaration of Competing Interest

The authors declare that they have no known competing financial interests or personal relationships that could have appeared to influence the work reported in this paper.

Acknowledgments

This work was supported by the Conselleria d'Educació, Investigació, Cultura I Esport: SUBVENCIONES PARA LA REALIZACIÓN DE ESTANCIAS DE PERSONAL INVESTIGADOR DOCTOR EN EMPRESAS DE LA COMUNITAT VALENCIANA: AEST-2018.

References

[1] IEA, *Electiricity Market Report 2023*. en Electricity Market Report, no. 2023. IEA, 2023. Accedido: 13 de diciembre de 2023. [En línea]. Disponible en: https://www.iea.org/reports/electricity-market-report-2023.
[2] OECD, *World Energy Outlook 2023*. en World Energy Outlook. OECD, 2023. doi: 10.1787/827374a6-en.
[3] IRENA, *Renewable Power Generation Costs in 2019*. en Renewable Power Generation Costs, no. 2020. Abu Dhabi: International Renewable Energy Agency, 2020.
[4] Z. Hua, C. Ma, J. Lian, X. Pang, W. Yang, Optimal capacity allocation of multiple solar trackers and storage capacity for utility-scale photovoltaic plants considering output characteristics and complementary demand, Appl. Energy 238 (2019) 721–733, https://doi.org/10.1016/j.apenergy.2019.01.099.
[5] S. Seme, B. Štumberger, M. Hadžiselimović, K. Sredenšek, Solar photovoltaic tracking systems for electricity generation: A review, Energies 13 (16) (2020) 4224, https://doi.org/10.3390/en13164224.
[6] L.M. Fernández-Ahumada, J. Ramírez-Faz, R. López-Luque, M. Varo-Martínez, I. M. Moreno-García, F. Casares De La Torre, Influence of the design variables of photovoltaic plants with two-axis solar tracking on the optimization of the tracking and backtracking trajectory, Sol. Energy 208 (2020) 89–100, https://doi.org/10.1016/j.solener.2020.07.063.
[7] R. Singh, S. Kumar, A. Gehlot, Y.R. Pachauri, An imperative role of sun trackers in photovoltaic technology: A review, Renew, Sustain. Energy Rev. 82 (2018) 3263–3278, https://doi.org/10.1016/j.rser.2017.10.018.
[8] S. Abdallah, S. Nijmeh, Two axes sun tracking system with PLC control, Energy Convers. Manag. 45 (11–12) (2004) 1931–1939, https://doi.org/10.1016/j.enconman.2003.10.007.
[9] A. Dolara, F. Grimaccia, S. Leva, M. Mussetta, R. Faranda, M. Gualdoni, Performance analysis of a single-axis tracking PV system, IEEE J. Photovolt. 2 (4) (2012) 524–531, https://doi.org/10.1109/JPHOTOV.2012.2202876.
[10] S. Seme, et al., Dual-axis photovoltaic tracking system – Design and experimental investigation, Energy 139 (2017) 1267–1274, https://doi.org/10.1016/j.energy.2017.05.153.
[11] C. Sungur, Multi-axes sun-tracking system with PLC control for photovoltaic panels in Turkey, Renew, Energy 34 (4) (2009) 1119–1125, https://doi.org/10.1016/j.renene.2008.06.020.
[12] H.R. Ghosh, N.C. Bhowmik, M. Hussain, Determining seasonal optimum tilt angles, solar radiations on variously oriented, single and double axis tracking surfaces at Dhaka, Renew. Energy 35 (6) (2010) 1292–1297, https://doi.org/10.1016/j.renene.2009.11.041.
[13] T. Maatallah, S. El Alimi, S.B. Nassrallah, Performance modeling and investigation of fixed, single and dual-axis tracking photovoltaic panel in Monastir city, Tunisia, Renew. Sustain. Energy Rev. 15 (8) (2011) 4053–4066, https://doi.org/10.1016/j.rser.2011.07.037.
[14] R.G. Vieira, F.K.O.M.V. Guerra, M.R.B.G. Vale, M.M. Araújo, Comparative performance analysis between static solar panels and single-axis tracking system on a hot climate region near to the equator, Renew. Sustain. Energy Rev. 64 (2016) 672–681, https://doi.org/10.1016/j.rser.2016.06.089.
[15] Z. Zhen, et al., The effects of inclined angle modification and diffuse radiation on the sun-tracking photovoltaic system, IEEE J. Photovolt. 7 (5) (2017) 1410–1415, https://doi.org/10.1109/JPHOTOV.2017.2715718.
[16] A. Bahrami, C.O. Okoye, U. Atikol, The effect of latitude on the performance of different solar trackers in Europe and Africa, Appl. Energy 177 (2016) 896–906, https://doi.org/10.1016/j.apenergy.2016.05.103.
[17] G. Quesada, L. Guillon, D.R. Rousse, M. Mehrtash, Y. Dutil, P.-L. Paradis, Tracking strategy for photovoltaic solar systems in high latitudes, Energy Convers. Manag. 103 (2015) 147–156, https://doi.org/10.1016/j.enconman.2015.06.041.
[18] J. Antonanzas, R. Urraca, F.J. Martinez-de-Pison, F. Antonanzas, Optimal solar tracking strategy to increase irradiance in the plane of array under cloudy conditions: A study across Europe, Sol. Energy 163 (2018) 122–130, https://doi.org/10.1016/j.solener.2018.01.080.
[19] L.M. Fernández-Ahumada, F.J. Casares, J. Ramírez-Faz, R. López-Luque, Mathematical study of the movement of solar tracking systems based on rational models, Sol. Energy 150 (2017) 20–29, https://doi.org/10.1016/j.solener.2017.04.006.
[20] N.A. Kelly, T.L. Gibson, Improved photovoltaic energy output for cloudy conditions with a solar tracking system, Sol. Energy 83 (11) (2009) 2092–2102, https://doi.org/10.1016/j.solener.2009.08.009.
[21] L. Narvarte, E. Lorenzo, Tracking and ground cover ratio, Prog. Photovolt. Res. Appl. 16 (8) (2008) 703–714, https://doi.org/10.1002/pip.847.
[22] Y.-M., Saint-Drenan, T. Barbier, Data-analysis and modelling of the effect of inter-row shading on the power production of photovoltaic plants, Sol. Energy 184 (2019) 127–147, https://doi.org/10.1016/j.solener.2019.03.086.
[23] K. Anderson, M. Mikofski, Slope-Aware Backtracking for Single-Axis Trackers , NREL/TP–5K00-76626, 1660126, MainId:7307, jul. 2020. doi: 10.2172/1660126.
[24] F.J. Gómez-Uceda, I.M. Moreno-Garcia, J.M. Jiménez-Martínez, R. López-Luque, L. M. Fernández-Ahumada, Analysis of the influence of terrain orientation on the design of pv facilities with single-axis trackers, Appl. Sci. 10 (23) (2020) 8531, https://doi.org/10.3390/app10238531.
[25] M.H. De Sá Campos, C. Tiba, npTrack: A n-Position Single Axis Solar Tracker Model for Optimized Energy Collection, Energies 14, 4 (2021) 925, https://doi.org/10.3390/en14040925.
[26] F. Sallaberry, R. Pujol-Nadal, M. Larcher, M.H. Rittmann-Frank, Direct tracking error characterization on a single-axis solar tracker, Energy Convers. Manag. 105 (2015) 1281–1290, https://doi.org/10.1016/j.enconman.2015.08.081.
[27] L. San José, G. Vallerotto, R. Herrero, R. Núñez, I. Antón, On-site characterization of misalignments between concentrator photovoltaic modules installed on trackers, Sol. Energy 244 (2022) 379–385, https://doi.org/10.1016/j.solener.2022.08.063.
[28] Y. Shao, et al., Methods of analyzing the error and rectifying the calibration of a solar tracking system for high-precision solar tracking in orbit, Remote Sens. 15 (8) (2023) 2213, https://doi.org/10.3390/rs15082213.
[29] A. Barbón, P. Fortuny Ayuso, L. Bayón, C.A. Silva, Experimental and numerical investigation of the influence of terrain slope on the performance of single-axis trackers, Appl. Energy 348 (2023), https://doi.org/10.1016/j.apenergy.2023.121524.
[30] K. Anderson, Maximizing Yield with Improved Single-Axis Backtracking on Cross-Axis Slopes , en *2020 47th IEEE Photovoltaic Specialists Conference (PVSC)*, Calgary, AB, Canada: IEEE, jun. 2020, pp. 1466-1471. doi: 10.1109/PVSC45281.2020.9300438.
[31] R. Perez, P. Ineichen, R. Seals, J. Michalsky, R. Stewart, Modeling daylight availability and irradiance components from direct and global irradiance, Sol. Energy 44 (5) (1990) 271–289, https://doi.org/10.1016/0038-092X(90)90055-H.
[32] P. Ineichen, R. Perez, R.D. Seal, E.L. Maxwell, A. Zalenka, Dynamic global-to-direct irradiance conversion models, ASHRAE Trans. 98 (1) (1992) 354–369.